determining how sustainable deltas become in the long term. Investments that manage the drivers of RSLR, rather than its symptoms, will be necessary to sustain deltas. Although the time horizons are long, acting now is essential, given that rehabilitation will be difficult (if not impossible) to achieve once ground is lost to rising seas.

REFERENCES AND NOTES

1. C. D. Woodroffe, R. J. Nicholls, Y. Saito, Z. Chen, S. L. Goodbred, in *Global Change and Integrated Coastal Management*, N. Harvey, Ed. (Springer Science and Business Media, Dordrecht, Netherlands, 2006), pp. 277–314.
2. M. VanKoningsveld, J. P. M. Mulder, M. J. F. Stive, L. VanDerValk, A. W. VanDerWeck, *J. Coast. Res.* **242**, 367–379 (2008).
3. J. W. Day Jr. *et al.*, *Science* **315**, 1679–1684 (2007).
4. J. P. M. Syvitski, Y. Saito, *Global Planet. Change* **57**, 261–282 (2007).
5. J. P. Ericson, C. J. Vorosmarty, S. L. Dingman, L. G. Ward, M. Meybeck, *Global Planet. Change* **50**, 63–82 (2006).
6. C. J. Vörösmarty *et al.*, *Global Planet. Change* **39**, 169–190 (2003).
7. H. J. Wang *et al.*, *Global Planet. Change* **57**, 331–354 (2007).
8. J. P. M. Syvitski *et al.*, *Nat. Geosci.* **2**, 681–686 (2009).
9. S. Mazzotti, A. Lambert, M. Van der Kooij, A. Mainville, *Geology* **37**, 771–774 (2009).
10. S. Higgins, I. Overeem, A. Tanaka, J. P. M. Syvitski, *Geophys. Res. Lett.* **40**, 3898–3902 (2013).
11. T. R. Knutson *et al.*, *Nat. Geosci.* **3**, 157–163 (2010).
12. B. P. Horton, S. Rahmstorf, S. E. Engelhart, A. C. Kemp, *Quat. Sci. Rev.* **84**, 1–6 (2014).
13. F. G. Renaud *et al.*, *Curr. Opin. Environ. Sustain.* **5**, 644–654 (2013).
14. J. W. Day, M. Moerschbaecher, D. Pimentel, C. Hall, A. Yáñez-Arancibia, *Ecol. Eng.* **65**, 33–48 (2014).
15. S. Temmerman *et al.*, *Nature* **504**, 79–83 (2013).
16. National Research Council, *Landscapes on the Edge: New Horizons for Research on Earth's Surface* (National Academies Press, Washington, DC, 2010).
17. N. Brooks, W. N. Adger, P. M. Kelly, *Glob. Environ. Change* **15**, 151–163 (2005).
18. V. Gornitz, *Palaeogeogr. Palaeoclimatol. Palaeoecol.* **89**, 379–398 (1991).
19. B. S. Halpern *et al.*, *Science* **319**, 948–952 (2008).
20. C. J. Vörösmarty *et al.*, *Nature* **467**, 555–561 (2010).
21. D. L. Balk *et al.*, *Adv. Parasitol.* **62**, 119–156 (2006).
22. S. Cutter, *Prog. Hum. Geogr.* **20**, 529–539 (1996).
23. C. J. Vörösmarty, L. B. de Guenni, W. M. Wollheim, B. Pellerin, D. Bjerklie, M. Cardoso, C. D'Almeida, P. Green, L. Colon, *Philos. Trans. R. Soc. London Ser. A* **371** (2013); http://rsta.royalsocietypublishing.org/content/371/2002/20120408.
24. Y. Budiyono, J. Aerts, J. Brinkman, M. A. Marfai, P. Ward, *Nat. Hazards* **75**, 389–413 (2015).
25. Y. C. E. Yang, P. A. Ray, C. M. Brown, A. F. Khalil, W. H. Yu, *Nat. Hazards* **75**, 2773–2791 (2015).
26. T. Bucx, M. Marchand, B. Makaske, C. van de Guchte, *Comparative Assessment of the Vulnerability and Resilience of 10 Deltas – Synthesis Report* (Delta Alliance report number 1, Delta Alliance International, Delft-Wageningen, Netherlands, 2010).
27. P. Kabat *et al.*, *Nat. Geosci.* **2**, 450–452 (2009).
28. U.S. Energy Information Administration, *Annual Energy Outlook 2015* (DOE/EIA-0383, U.S. Department of Energy, Washington, DC, 2015).
29. R. Dankers *et al.*, *Proc. Natl. Acad. Sci. U.S.A.* **111**, 3257–3261 (2014).
30. S. Jevrejeva, J. C. Moore, A. Grinsted, A. P. Matthews, G. Spada, *Global Planet. Change* **113**, 11–22 (2014).
31. K. C. Seto, B. Güneralp, L. R. Hutyra, *Proc. Natl. Acad. Sci. U.S.A.* **109**, 16083–16088 (2012).
32. C. Kuenzer *et al.*, *Sustain. Sci.* **8**, 565–584 (2013).
33. C. Zarfl, A. E. Lumsdon, J. Berlekamp, L. Tydecks, K. Tockner, *Aquat. Sci.* **77**, 161–170 (2015).

ACKNOWLEDGMENTS

Data are available as supplementary materials on *Science* Online. This work was supported by NASA (Land Cover/Land Use Change Program grant NNX12AD28G) and NSF (Belmont Forum Coastal Vulnerability awards 1343458 and 1342944, and Dynamics of Coupled Natural and Human Systems award 1115025). The authors report no conflicts of interest. The authors thank B. Fekete and P. Green for helpful comments on the manuscript.

SUPPLEMENTARY MATERIALS

www.sciencemag.org/content/349/6248/638/suppl/DC1
Materials and Methods
Figs. S1 to S4
Tables S1 to S3
References (*34*–*52*)

15 April 2015; accepted 30 June 2015
10.1126/science.aab3574

HUMORAL IMMUNITY

T cell help controls the speed of the cell cycle in germinal center B cells

Alexander D. Gitlin,[1] Christian T. Mayer,[1] Thiago Y. Oliveira,[1] Ziv Shulman,[1] Mathew J. K. Jones,[2] Amnon Koren,[4] Michel C. Nussenzweig[1,3]*

The germinal center (GC) is a microanatomical compartment wherein high-affinity antibody-producing B cells are selectively expanded. B cells proliferate and mutate their antibody genes in the dark zone (DZ) of the GC and are then selected by T cells in the light zone (LZ) on the basis of affinity. Here, we show that T cell help regulates the speed of cell cycle phase transitions and DNA replication of GC B cells. Genome sequencing and single-molecule analyses revealed that T cell help shortens S phase by regulating replication fork progression, while preserving the relative order of replication origin activation. Thus, high-affinity GC B cells are selected by a mechanism that involves prolonged dwell time in the DZ where selected cells undergo accelerated cell cycles.

Antibodies elicited during T cell–dependent immune responses undergo substantial increases in affinity over time (*1*). This phenomenon, known as affinity maturation, takes place in the germinal center (GC), where antigen-specific B cells diversify their antibodies by somatic hypermutation (*2*) and undergo selective clonal expansion (*3*–*7*). Together, these events are essential to the development of effective antibody responses.

GC B cells bearing antibody variants with higher affinity are selectively expanded during iterative rounds of migration between the dark zone (DZ), where they proliferate and hypermutate, and the light zone (LZ), where they capture antigen displayed on the surface of follicular dendritic cells (*8*–*11*). By binding and internalizing more antigen in the LZ, high-affinity clones present more peptide–major histocompatibility complex II (MHCII) and thereby elicit greater help from $CD4^+$ T follicular helper cells (*11*, *12*). The magnitude of T cell help determines how long B cells reside in the DZ, which provides selected cells more time to proliferate and expand in between rounds of competition in the LZ (*13*). Whether this mechanism alone explains how high-affinity B cells are selected remains unknown.

[1]Laboratory of Molecular Immunology, The Rockefeller University, New York, NY 10065, USA. [2]Molecular Biology Program, Memorial Sloan-Kettering Cancer Center, 1275 York Avenue, New York, NY 10065, USA. [3]Howard Hughes Medical Institute (HHMI), The Rockefeller University, New York, NY 10065, USA. [4]Department of Genetics, Harvard Medical School, Boston, MA 02115, USA.
***Corresponding author. E-mail: nussen@rockefeller.edu**

To explore additional mechanisms that could contribute to selection, we used an adoptive transfer model in which antigen presentation by a subset of GC B cells can be acutely and selectively increased (*11*, *14*, *15*). B cells carrying a knock-in antigen receptor specific for the hapten 4-hydroxy-3-nitrophenylacetyl (NP) (B1-8^{hi}) were transferred into ovalbumin (OVA)–primed wild-type mice that were boosted with NP-OVA. Whereas the majority of transferred B1-8^{hi} B cells were $DEC205^{-/-}$ (~85%), a subset (~15%) of the B1-8^{hi} B cells were $DEC205^{+/+}$ (*10*, *16*). DEC205 is an endocytic receptor expressed by GC B cells that delivers antigen to MHCII processing compartments (*14*). Targeting DEC205 with an antibody that is fused at its C terminus to OVA (αDEC–OVA), but not the irrelevant control antigen *Plasmodium falciparum* circumsporozoite protein (αDEC-CS) (*17*), increases the amount of cognate peptide–MHCII displayed on the surface of B1-8^{hi} $DEC205^{+/+}$ GC B cells, which leads to their selective expansion (*11*–*13*).

To determine whether B cells receiving high levels of T cell help show a specific change in gene expression, we compared DZ cells in the G_1 phase of the cell cycle from αDEC-OVA– and control αDEC-CS–treated GCs, using a fluorescent ubiquitination-based cell cycle indicator ($Fucci^{tg}$) (fig. S1) (*18*, *19*). RNA sequencing revealed that T cell–mediated selection produced a statistically significant increase in gene expression programs associated with the cell cycle, metabolism (including the metabolism of nucleotides), and genes downstream of c-Myc and the E2F transcription factors (Fig. 1, A and B, and fig. S2). Finding an

increase in expression of c-Myc target genes is in agreement with the observation that c-Myc is induced by T cell help in the GC (*20*, *21*). E2F transcription factors are principal drivers of the cell cycle and are activated by cyclin-dependent kinase (CDK) phosphorylation of the retinoblastoma (Rb) protein (*22*, *23*). Consistent with this, Rb was highly phosphorylated in GC B cells receiving enhanced T cell help (Fig. 1C). E2F and c-Myc are crucial drivers of cell cycle phase transitions; moreover, their activation regulates nucleotide metabolism and controls DNA replication dynamics (*23*–*26*), which suggests that T cell help might control the cell cycle dynamics of selected GC B cells in vivo.

To examine cell cycle progression, mice were pulsed sequentially with the nucleoside analog 5-ethynyl-2′-deoxyuridine (EdU) followed 1 hour later by 5-bromo-2′-deoxyuridine (BrdU), and GC B cells were then stained for DNA content (Fig. 2A and fig. S3) (*13*). At 0.5 hours after the BrdU pulse, early S-phase cells were labeled as $EdU^{-}BrdU^{+}$ and had replicated only a small amount of their genome, which made their DNA content similar to that of G_1 cells (Fig. 2, A and B). By contrast, mid/late S-phase cells were labeled as $EdU^{+}BrdU^{+}$, and post–S phase cells (labeled as $EdU^{+}BrdU^{-}$) were either in G_2/M phase or in the G_1 phase of the next cell cycle (Fig. 2, A and B). Under control conditions (αDEC-CS), B1-8^{hi} $DEC205^{+/+}$ and B1-8^{hi} $DEC205^{-/-}$ post–S phase GC B cells were similarly distributed between G_2/M and G_1, which indicated equivalent rates of progression through the G_2/M phases of the cell cycle (Fig. 2C). By contrast, inducing selection by αDEC–OVA resulted in rapid progression through G_2/M and return to G_1 (Fig. 2C). Thus, T cell–mediated selection accelerates progression through G_2/M.

To examine S-phase dynamics, we followed GC B cells 2.5 and 5 hours after the EdU/BrdU double-pulse described above. At 2.5 hours, $EdU^{-}BrdU^{+}$ cells, which were in early S phase at 0.5 hours, had progressed into mid/late-S phase as determined by DNA content (Fig. 2, D and E). With only these two additional hours to replicate their genomes, selected GC B cells accumulated more DNA content and had therefore replicated their genomes at a faster rate than control cells obtained from αDEC-CS–treated mice (Fig. 2D and fig. S4). After 5 hours, nearly half of control cells that were labeled in early S phase ($EdU^{-}BrdU^{+}$) had completed S phase and were in G_2/M or G_1 (Fig. 2E). Selection significantly accelerated progression through S phase, as a far greater fraction of B1-8^{hi} $DEC205^{+/+}$ GC cells targeted with αDEC–OVA completed DNA replication in 5 hours than did cotransferred B1-8^{hi} $DEC205^{-/-}$ GC cells (Fig. 2F). We conclude that T cells induce accelerated progression of selected GC B cells through the S and G_2/M phases of the cell cycle.

To determine whether accelerated progression through the cell cycle is also a feature of polyclonal GC responses, we examined the response to NP in C57BL/*6* mice. High-affinity clones in NP-specific GCs carry a tryptophan-to-leucine mutation at position *33* (W33L) or a lysine-to-arginine mutation at position *59* (K59R) in the V_H186.2 antibody gene (*27*, *28*). Two weeks after immunization with NP-OVA, mice were pulsed with EdU, followed 30 min later by a large dose of BrdU to inhibit further EdU uptake (fig. S5). After 3.25 hours, EdU^{+} GC cells were separated into two distinct populations on the basis of DNA content (Fig. 3A): (i) EdU^{+} cells in S/G_2/M that represent a mixed population that initiated S phase at the time of EdU injection and/or progressed slowly through S/G_2/M; and (ii) EdU^{+} cells in G_1 that were close to completing S phase during the EdU injection and/or progressed rapidly through S/G_2/M. If high-affinity GC B cells progress through the cell cycle at an accelerated rate, then they should be enriched in the EdU^{+} G_1 population. Sequencing the V_H186.2 genes of these cells revealed that EdU^{+} G_1 cells were significantly enriched in high-affinity clones compared with EdU^{+} S/G_2/M cells (Fig. 3, B and C). Thus, affinity-enhancing mutations in the polyclonal GC are associated with rapid progression through S/G_2/M.

Once a GC B cell has entered the cell cycle, S phase occupies most of the time it takes for the cell to divide (Fig. 2) (*13*). We therefore sought to understand how T cell help accelerates progression through S phase. Control of S-phase length is a well-documented phenomenon during embryonic development (*29*). In this context, S-phase control operates at the level of initiation of DNA replication; rapid S phases are caused by an increased number of synchronously fired replication origins (*30*–*33*).

To evaluate the dynamics of DNA replication initiation, we sorted and sequenced the genomes of B1-8^{hi} $DEC205^{+/+}$ GC B cells in G_1 and S phase under control conditions or during their selective expansion (fig. S6, A and B). In a population of S-phase cells, genomic sites that replicate early have higher copy number than regions that are replicated later during S phase. Thus, by analyzing the relative copy number of DNA sequences along chromosomes in S-phase cells compared with G_1-phase cells, we obtained genome-wide profiles of DNA replication timing (*34*, *35*). The relative timing of DNA replication among selected and nonselected GC B cells was essentially identical, with the same locations and activation times of origins throughout the genome [correlation coefficient (r) = 0.98] (Fig. 4, A and B, and fig. S6C). Thus, T cell help accelerates S phase by proportionally condensing the replication timing program, while maintaining the overall dynamics of DNA replication albeit on a shorter time scale.

Elevated c-Myc, CDK activity, and nucleotide metabolism can increase the speed of DNA

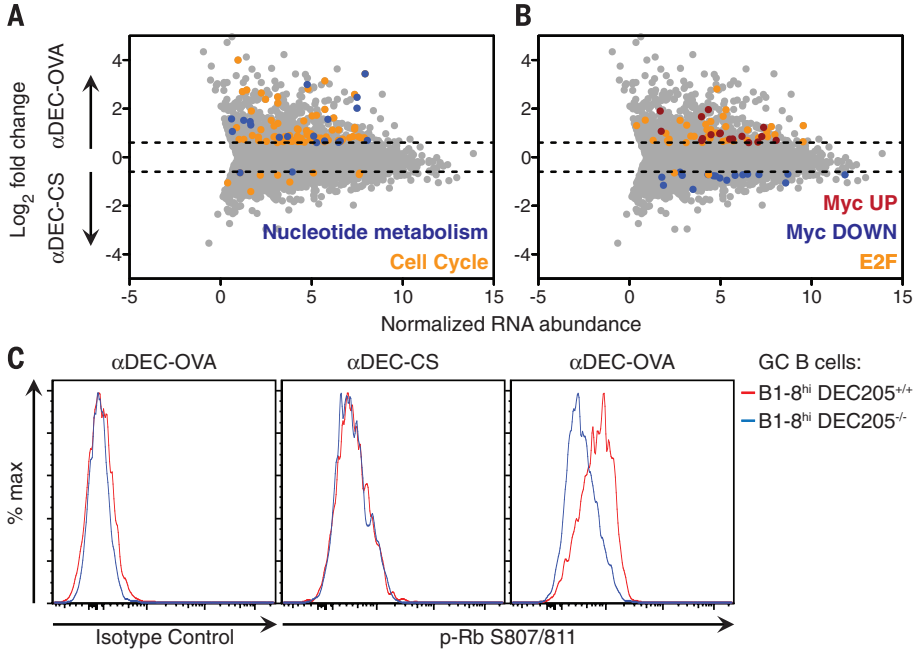

Fig. 1. T cell help regulates cell cycle and metabolic gene expression programs in selected GC B cells. (**A** and **B**) RNA sequencing analysis showing genes up- or down-regulated by a fold-change of at least 0.6 (log_2) upon treatment with αDEC-OVA or αDEC-CS. For clarity, enriched gene sets according to curated reactome gene sets (A) and transcription factor target genes (B) are shown separately. (**C**) Histograms showing intracellular levels of Rb phosphorylation in B1-8^{hi} $DEC205^{+/+}$ and B1-8^{hi} $DEC205^{-/-}$ GC B cells from mice treated 2 days earlier with αDEC-OVA or αDEC-CS. Results represent two (A and B) or three (C) independent experiments with n = 4 to 5 mice per condition for each experiment.

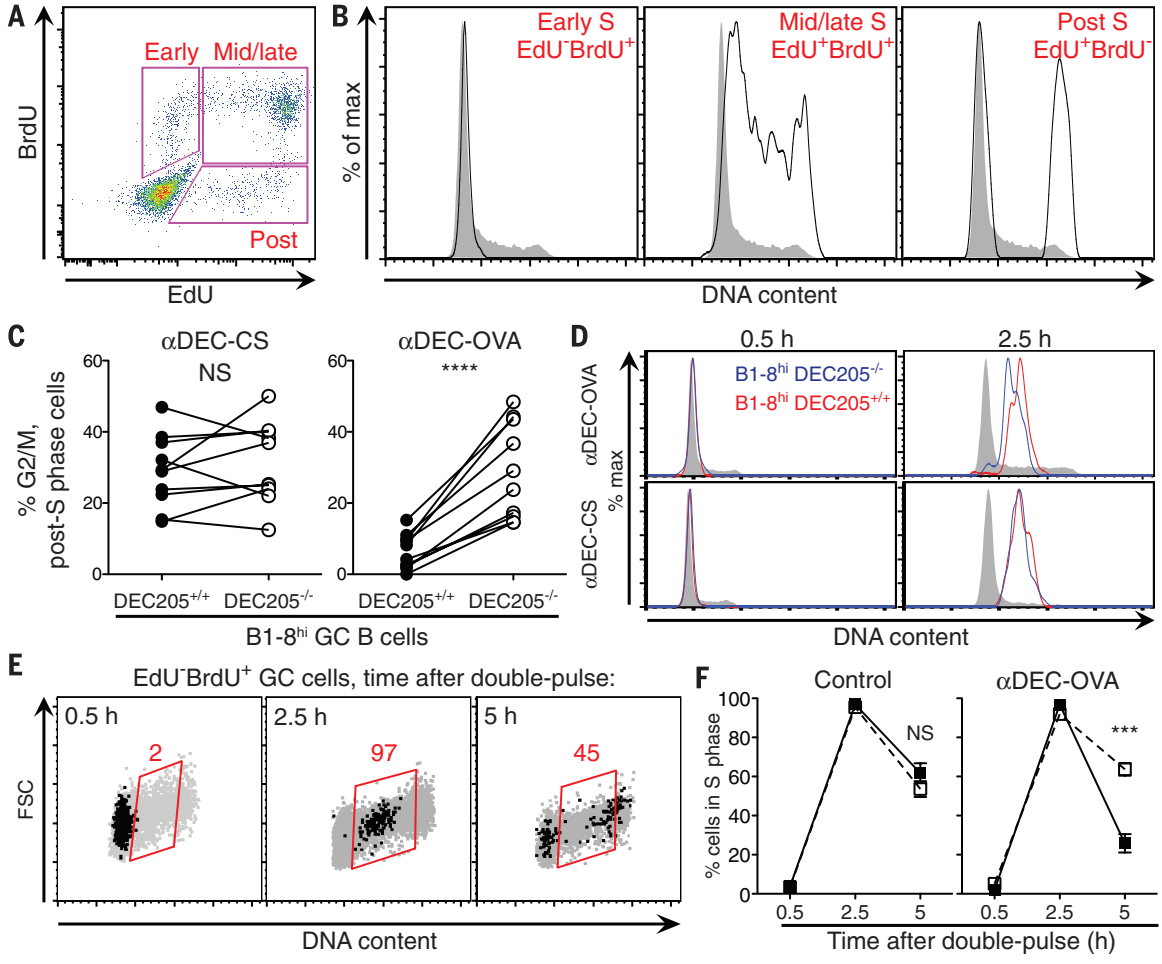

Fig. 2. T cell help regulates progression through S and G_2/M phases during selection. (**A**) Mice were injected with EdU intravenously followed 1 hour later by BrdU and then analyzed by flow cytometry 0.5 hours later. (**B**) Representative histograms displaying DNA content among all GC B cells (gray) and gated populations (black) shown in (A). (**C**) Mean fraction of cells in G_2/M as determined by DNA content among EdU^+BrdU^- (post–S phase) B1-8^{hi} $DEC205^{+/+}$ and B1-8^{hi} $DEC205^{-/-}$ GC B cells treated with αDEC-OVA or αDEC-CS (control) 2 days earlier. Lines connect indicated cell populations from the same animal. (**D**) Histograms showing progressive accumulation of DNA content among EdU^-BrdU^+ GC B cells from 0.5 to 2.5 hours after EdU/BrdU double pulse. (**E**) Flow cytometry plots showing time course of cell cycle progression of EdU^-BrdU^+ cells (black dots) at 0.5, 2.5, and 5 hours after double-pulse labeling. Gray dots represent all GC B cells in the same mice. Red values represent fraction in S-phase gate. (**F**) Mean fraction of GC B cells in S-phase gate among EdU^-BrdU^+ B1-8^{hi} $DEC205^{+/+}$ (black squares) and B1-8^{hi} $DEC205^{-/-}$ (white squares) cells as determined by DNA content at 0.5, 2.5, and 5 hours after double-pulse labeling in mice treated 2 days earlier with αDEC-OVA or either PBS or αDEC-CS (control). Error bars represent SEM. Two-tailed paired *t* test was used in (C) and two-tailed Mann-Whitney test in (F). $^{****}P < 0.0001$. $^{***}P = 0.0002$. Experiments represent two or three independent experiments with 7 to 10 mice total for each time point and condition.

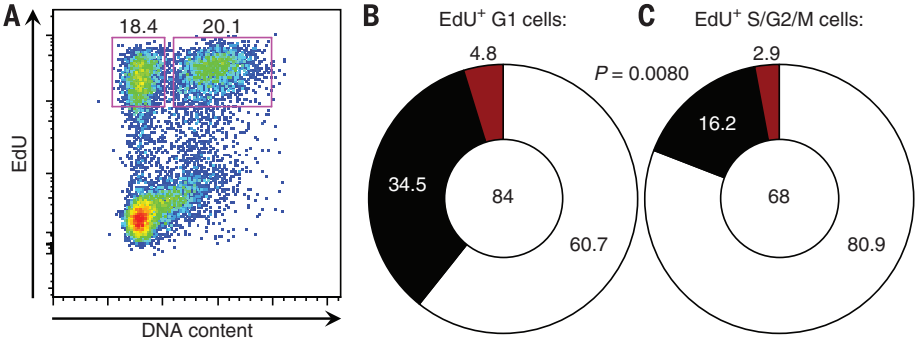

Fig. 3. Affinity-enhancing mutations in polyclonal GCs are associated with accelerated S/G_2/M progression. (**A**) WT mice were immunized with NP-OVA and 14 days later were administered EdU for 0.5 hours before BrdU. At 3.25 hours after BrdU administration, EdU^+ G_1 cells and EdU^+ S/G_2/M GC B cells were sorted and analyzed for affinity-enhancing mutation in VH186.2 genes. (**B** and **C**) Pie charts show frequency of $W33L^+$ (black) and $K59R^+$ (red) clones among VH186.2 sequences within EdU^+ G_1 (B) and EdU^+ S/G_2/M (C) GC B cells. One sequence was doubly positive for the W33L and K59R mutations and was counted within the black slice in (C). Total number of clones analyzed is shown in center. *P* value was determined using Fisher's exact test. Results are pooled from two independent experiments with 10 mice each.

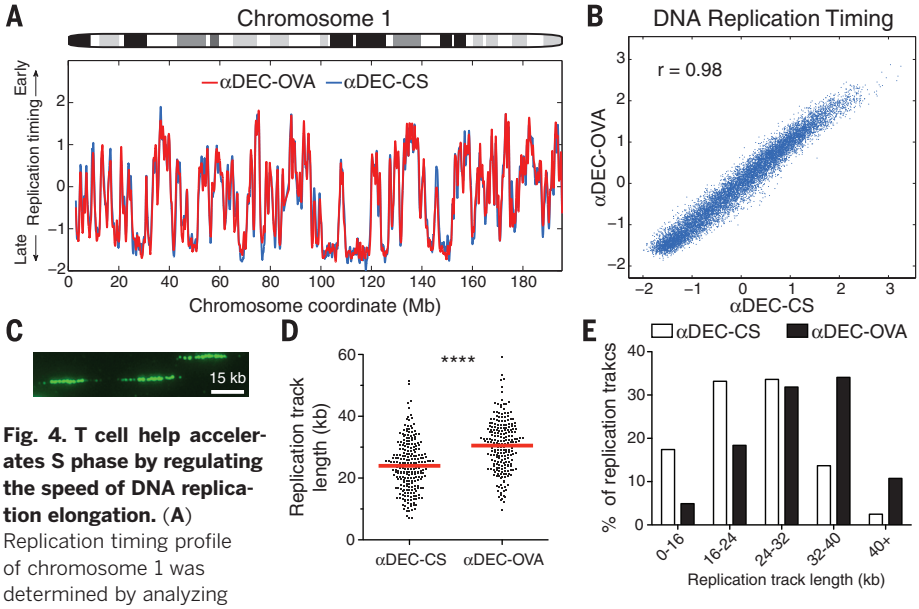

Fig. 4. T cell help accelerates S phase by regulating the speed of DNA replication elongation. (**A**) Replication timing profile of chromosome 1 was determined by analyzing the ratio of DNA copy number between sorted S and G_1 phase B1-8^{hi} DEC205$^{+/+}$ GC B cells treated with αDEC-CS or αDEC-OVA 2 days earlier. (**B**) Genome-wide correlation between replication timing in the two conditions. (**C**) Representative IdU-labeled DNA fibers are shown. (**D**) Replication track lengths from αDEC-CS or αDEC-OVA–treated B1-8^{hi} DEC205$^{+/+}$ GC B cells. Each data point represents an IdU-labeled track, and red lines represent mean values. Results are pooled from two independent experiments and involve >220 measured fibers in total for each condition. (**E**) Distribution of replication track lengths. ****P < 0.0001, two-tailed Mann-Whitney test.

replication fork progression in tissue culture cells, yet a physiological role for this mechanism has not been documented (*26*, *36*, *37*). Because T cell help produces similar molecular changes in selected GC B cells, we examined DNA replication forks by single-molecule analyses (*38*). For this purpose, αDEC-OVA or control αDEC-CS–treated mice were pulsed with the nucleoside analog 5-iodo-2′-deoxyuridine (IdU) (fig. S6D). GC B cells were then isolated by cell sorting and processed to measure the lengths of DNA replication tracks in individual molecules (Fig. 4C). Selection resulted in an increase in the average length of replication tracks and altered the distribution of replication track lengths, which indicated that T cell help regulates DNA replication by increasing the speed of individual DNA replication forks (Fig. 4, D and E) (P < 0.0001).

The GC imparts protective immunity by selectively expanding high-affinity B cells, yet the mechanisms whereby such clones come to dominate the GC population have been obscure (*3*, *4*). T cells discern among GC B cells on the basis of cell surface peptide–MHCII levels and transduce signal(s) that regulate the amount of time selected cells spend proliferating in the DZ (*8*, *11*–*13*). Thus, T cell help influences the choice that a recently divided GC B cell in G_1 must make in the DZ: either to reenter another S phase or, instead, to return to the LZ (*13*). Our results indicate that T cell–mediated selection extends beyond this mode of regulation and accelerates progression through the entire cell cycle in selected GC B cells. Thus, the regulatory effects transduced by T cells work in concert to induce selected GC B cells to spend a longer period of time in the DZ, where they proliferate at a faster rate.

There are few examples of physiological regulation of cell cycle speed in eukaryotes, and, to our knowledge, none known that involve directed signaling by one cell type to another (*29*). High levels of replication factors and CDK activity in the early embryo synchronize initiation from a greater number of origins to increase the rate of cell division (*31*, *39*). By contrast, during B cell selection, T cell help induces higher levels of critical regulators of the cell cycle (c-Myc and CDK) and nucleotide metabolism to accelerate DNA replication elongation, while preserving the temporal order and the number of initiation events throughout the genome. We conclude that selection in the GC involves dynamic regulation of genome replication in S phase, the longest phase of the committed cell cycle.

REFERENCES AND NOTES

1. H. N. Eisen, G. W. Siskind, *Biochemistry* **3**, 996–1008 (1964).
2. M. Muramatsu *et al.*, *Cell* **102**, 553–563 (2000).
3. C. Berek, A. Berger, M. Apel, *Cell* **67**, 1121–1129 (1991).
4. J. Jacob, G. Kelsoe, K. Rajewsky, U. Weiss, *Nature* **354**, 389–392 (1991).
5. C. Kocks, K. Rajewsky, *Proc. Natl. Acad. Sci. U.S.A.* **85**, 8206–8210 (1988).
6. K. Rajewsky, *Nature* **381**, 751–758 (1996).
7. G. D. Victora, M. C. Nussenzweig, *Annu. Rev. Immunol.* **30**, 429–457 (2012).
8. C. D. Allen, T. Okada, H. L. Tang, J. G. Cyster, *Science* **315**, 528–531 (2007).
9. A. E. Hauser *et al.*, *Immunity* **26**, 655–667 (2007).
10. T. A. Schwickert *et al.*, *Nature* **446**, 83–87 (2007).
11. G. D. Victora *et al.*, *Cell* **143**, 592–605 (2010).
12. Z. Shulman *et al.*, *Science* **345**, 1058–1062 (2014).
13. A. D. Gitlin, Z. Shulman, M. C. Nussenzweig, *Nature* **509**, 637–640 (2014).
14. W. Jiang *et al.*, *Nature* **375**, 151–155 (1995).
15. A. O. Kamphorst, P. Guermonprez, D. Dudziak, M. C. Nussenzweig, *J. Immunol.* **185**, 3426–3435 (2010).
16. T. A. Shih, M. Roederer, M. C. Nussenzweig, *Nat. Immunol.* **3**, 399–406 (2002).
17. S. B. Boscardin *et al.*, *J. Exp. Med.* **203**, 599–606 (2006).
18. A. Sakaue-Sawano *et al.*, *Cell* **132**, 487–498 (2008).
19. Y. Aiba *et al.*, *Proc. Natl. Acad. Sci. U.S.A.* **107**, 12192–12197 (2010).
20. D. Dominguez-Sola *et al.*, *Nat. Immunol.* **13**, 1083–1091 (2012).
21. D. P. Calado *et al.*, *Nat. Immunol.* **13**, 1092–1100 (2012).
22. S. P. Chellappan, S. Hiebert, M. Mudryj, J. M. Horowitz, J. R. Nevins, *Cell* **65**, 1053–1061 (1991).
23. H. Z. Chen, S. Y. Tsai, G. Leone, *Nat. Rev. Cancer* **9**, 785–797 (2009).
24. C. V. Dang, *Cell* **149**, 22–35 (2012).
25. D. Dominguez-Sola, J. Gautier, *Cold Spring Harb. Perspect. Med.* **4**, a014423 (2014).
26. A. C. Bester *et al.*, *Cell* **145**, 435–446 (2011).
27. D. Allen, T. Simon, F. Sablitzky, K. Rajewsky, A. Cumano, *EMBO J.* **7**, 1995–2001 (1988).
28. K. Furukawa, A. Akasako-Furukawa, H. Shirai, H. Nakamura, T. Azuma, *Immunity* **11**, 329–338 (1999).
29. J. Nordman, T. L. Orr-Weaver, *Development* **139**, 455–464 (2012).
30. A. B. Blumenthal, H. J. Kriegstein, D. S. Hogness, *Cold Spring Harb. Symp. Quant. Biol.* **38**, 205–223 (1974).
31. C. Collart, G. E. Allen, C. R. Bradshaw, J. C. Smith, P. Zegerman, *Science* **341**, 893–896 (2013).
32. O. Hyrien, C. Maric, M. Méchali, *Science* **270**, 994–997 (1995).
33. S. L. McKnight, O. L. Miller Jr., *Cell* **12**, 795–804 (1977).
34. A. Koren *et al.*, *Cell* **159**, 1015–1026 (2014).
35. A. Koren *et al.*, *Am. J. Hum. Genet.* **91**, 1033–1040 (2012).
36. M. Anglana, F. Apiou, A. Bensimon, M. Debatisse, *Cell* **114**, 385–394 (2003).
37. J. Malínsky *et al.*, *J. Cell Sci.* **114**, 747–750 (2001).
38. D. A. Jackson, A. Pombo, *J. Cell Biol.* **140**, 1285–1295 (1998).
39. J. A. Farrell, A. W. Shermoen, K. Yuan, P. H. O'Farrell, *Genes Dev.* **26**, 714–725 (2012).

ACKNOWLEDGMENTS

We thank A. Miyawaki and T. Kurosaki for mice, T. Eisenreich for help with mouse colony management, K. Yao for technical help, J. Hurwitz and A. Farina for advice, B. Zhang and C. Zhao and the Rockefeller University Genomics Resource Center for assistance with high-throughput sequencing, K. Velinzon for assistance with cell sorting, and all members of the Nussenzweig laboratory for discussion. The data presented in this manuscript are tabulated in the main paper and in the supplementary materials. Supported by NIH Medical Scientist Training Program grant T32GM07739 and National Institute of Allergy and Infectious Diseases, NIH, grant 1F30AI109903-01 (A.D.G.); NIH grants AI037526-19 and AI072529-06 (M.C.N.); and the NIH Center for HIV/AIDS Vaccine Immunology and Immunogen Discovery (CHAVI-ID) 1UM1 AI100663-01 (M.C.N). Z.S. is a Human Frontiers of Science Program Fellow (reference LT000340/2011-L). C.T.M is an EMBO fellow (ALTF 456-2014) and is supported by the European Commission FP7 (Marie Curie Actions, EMBOCOFUND2012, GA-2012-600394). M.C.N. is an HHMI investigator. RNA sequencing data was deposited in the National Center for Biotechnology Information (NCBI), NIH, Gene Expression Omnibus (GEO) and is accessible through accession number GSE71295. Replication timing data was deposited in NCBI's Sequence Read Archive (SRA) and is accessible through accession number SRP061569.

SUPPLEMENTARY MATERIALS

www.sciencemag.org/content/349/6248/643/suppl/DC1
Materials and Methods
Figs. S1 to S6
References (*40*, *41*)

3 May 2015; accepted 8 July 2015
Published online 16 July 2015
10.1126/science.aac4919

T cell help controls the speed of the cell cycle in germinal center B cells

Alexander D. Gitlin *et al.*

Science **349**, 643 (2015);
DOI: 10.1126/science.aac4919